Clays and Clay Minerals, Vol. 41, No. 5, 537–550, 1993.

COMPOSITIONAL END MEMBERS AND THERMODYNAMIC COMPONENTS OF ILLITE AND DIOCTAHEDRAL ALUMINOUS SMECTITE SOLID SOLUTIONS

BARBARA RANSOM[1] AND HAROLD C. HELGESON

Department of Geology and Geophysics, University of California, Berkeley, California 94720

Abstract—Consideration of XRD, TEM, AEM, and analytical data reported in the literature indicates that dioctahedral aluminous smectite and illite form two separate solid solutions that differ chemically from one another primarily by the extent of Al substitution for Si, the amount of interlayer K, and the presence of interlayer H_2O. The data indicate that limited dioctahedral-trioctahedral and dioctahedral-vacancy compositional variations occur in both minerals. Excluding interlayer H_2O and based on a half unit cell [i.e., $O_{10}(OH)_2$], natural dioctahedral smectite and illite solid solutions fall within the compositional limits represented by $A_{0.3}R^{3+}_{1.9}Si_4O_{10}(OH)_2$-$AR^{2+}R^{3+}Si_4O_{10}(OH)_2$-$A_{0.25}R^{2+}_{0.3}R^{3+}_{1.8}Al_{0.25}Si_{3.75}O_{10}(OH)_2$ for smectites and $A_{0.8}R^{3+}_{1.5}Al_{0.5}Si_{3.5}O_{10}(OH)_2$-$A_{0.55}R^{2+}_{0.45}R^{3+}_{1.55}Al_{0.1}Si_{3.9}O_{10}(OH)_2$-$A_{0.9}R^{2+}_{0.3}R^{3+}_{1.8}Al_{0.9}Si_{3.1}O_{10}(OH)_2$ for illites, where A represents either monovalent cations or divalent cations expressed as their monovalent equivalent (e.g., $Ca^{2+}/2$); R^{2+} stands for the divalent cations Mg^{2+} and Fe^{2+}; and R^{3+} refers to the trivalent cations Al^{3+} and Fe^{3+}. Taking account of these compositional limits, smectite and illite solid solutions can be described in terms of nine and six thermodynamic components, respectively, all of which are consistent with both the law of definite proportions and the concept of a unit cell. Thermodynamic components that can be used to describe natural smectite solid solutions in terms of a half unit cell [i.e., $O_{10}(OH)_2$] can be expressed as $NaAl_3Si_3O_{10}(OH)_2$, $NaAl_3Si_3O_{10}(OH)_2 \cdot 4.5H_2O$, $Al_2Si_4O_{10}(OH)_2$, $Fe_2Si_4O_{10}(OH)_2$, $Mg_3Si_4O_{10}(OH)_2$, $Fe_3Si_4O_{10}(OH)_2$, $K_3AlSi_4O_{10}(OH)_2$, $KAl_3Si_3O_{10}(OH)_2$, and $Ca_{0.5}Al_3Si_3O_{10}(OH)_2$. Of these, $NaAl_3Si_3O_{10}(OH)_2 \cdot 4.5H_2O$ provides explicitly for the presence of interlayer H_2O in the mineral. Thermodynamic components representing illite solid solutions in natural systems can be written for a half unit cell as $KAl_3Si_3O_{10}(OH)_2$, $KMg_3AlSi_3O_{10}(OH)_2$, $KFe_3AlSi_3O_{10}(OH)_2$, $Al_2Si_4O_{10}(OH)_2$, $KFe_2AlSi_3O_{10}(OH)_2$, and $K_3AlSi_4O_{10}(OH)_2$. The calculations and observations summarized below indicate that neither smectite nor illite occur in nature as stoichiometric phases and that the two minerals do not form a mutual solid solution corresponding to mixed-layered illite/smectite.

Key Words—Clay minerals, Composition, End members, Illite, I/S clays, Mixed-layered clays, Smectite, Stoichiometry, Structural formula, Thermodynamic components, Thermodynamic status.

INTRODUCTION

Illite and the dioctahedral aluminous members of the smectite group are major constituents of sedimentary rocks and participants in many chemical reactions that occur during weathering and sediment diagenesis.[2] Accurate chemical representation of these two minerals is fundamental to prediction of their thermodynamic behavior in geochemical processes. Although the chemical and physical constitution of illite and smectite have received widespread attention, failure to document adequately the mineralogy of clay samples before computing structural formulas from combined X-ray diffraction (XRD) data and bulk chemical analyses has resulted in considerable confusion over the extent to which illite and smectite exhibit mutual solid solubility. For example, it can be seen in Figure 1 that extensive compositional overlap occurs among minerals designated in the literature as smectites, illites, and what are commonly called mixed-layered I/S clays. Although this overlap has been cited as evidence that smectite and illite form a mutual solid solution, it is not necessarily indicative of solid solution between them (Ransom and Helgeson, 1989; Warren and Ransom, 1992).[3] The purpose of the present communication is to determine accurate compositional limits of solid solubility in smectite and illite by critically analyzing compositional data reported in the literature in order to generate sets of thermodynamic components that can be used to describe the chemical interaction of illite and smectite with their mineralogic and aquatic environment.

Many smectite and illite analyses have been published over the past 50 years (Ross and Hendricks, 1945; Kerr *et al.*, 1950; Earley *et al.*, 1953; Yoder and Eugster, 1955; Foster, 1951, 1953, 1954; Hower and

[1] Current address: Geosciences Research Division 0220, Scripps Institution of Oceanography, University of California at San Diego, La Jolla, California 92093-0220.

[2] In accord with the classification system established by the AIPEA (Bailey *et al.*, 1984), the terms smectite and illite are used in the present communication to refer to two separate mineral groups that have specific crystallographic and chemical characteristics that distinguish the species in one group from those in the other.

[3] As discussed by Warren and Ransom (1992), compositional ambiguities in Figure 1 also arise in part from plotting the compositions of clay minerals that are not perfectly dioctahedral on coordinates which require them to be so.

Copyright © 1993, The Clay Minerals Society

https://doi.org/10.1346/CCMN.1993.0410503 Published online by Cambridge University Press

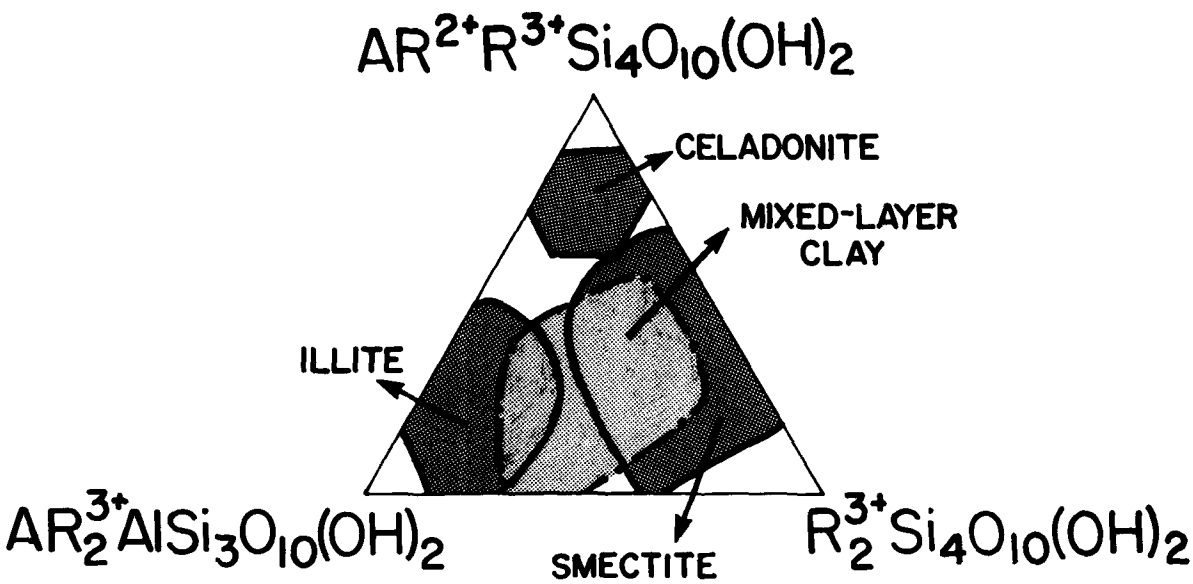


Figure 1. Fields of compositional variation for smectite, illite, celadonite, and mixed-layered clays reported by Weaver and Pollard (1973). The chemical formula groups at the apices of the triangle correspond to generic formulas in which A denotes monovalent cations or divalent cations expressed as their monovalent equivalent (e.g., $Ca^{2+}/2$), R^{2+} refers to the divalent cations Mg^{2+} and Fe^{2+}, and R^{3+} stands for the trivalent cations Al^{3+} and Fe^{3+}.

Mowatt, 1966; Schultz, 1969; Weaver and Pollard, 1973; Hower *et al.*, 1976; Grim and Guven, 1978; Brigatti and Poppi, 1981; Merino and Ransom, 1982; Inoue and Utada, 1983; Środoń and Eberl, 1984; Środoń *et al.*, 1986; Velde and Brusewitz, 1986; Nadeau and Bain, 1986; Guven, 1988; Newman and Brown, 1987; Warren and Curtis, 1989; Jiang *et al.*, 1990; and others). However, most of the resulting structural formulas were not generated from chemical analyses of single crystals, but rather from bulk compositions of clay samples that appear from XRD analyses to be composed solely of smectite or illite. It has been shown recently (Warren and Ransom, 1992) that XRD analysis alone cannot be used to characterize unambiguously the mineralogy of clay samples. For example, standard XRD analyses of powdered samples in the 35–40 micron size fraction cannot detect less than ~0.5 wt. % quartz or ~7 wt. % discrete illite grains in any given bulk sample (Pawloski, 1985). In addition, as the grain size of the minerals that are present in minor amounts in the sample decreases, the percentage that escapes detection by XRD increases (Till and Spears, 1969; Maniar and Cooke, 1987). In the clay size fraction of sediments, powder XRD techniques generally cannot detect accessory oxides and hydroxides at levels below ~5% of the total sample weight (Reynolds, 1980). Similarly, uncertainties in determining the concentrations of structurally similar 2:1 phyllosilicates in the sample can range up to 20% (Środoń, 1980). As a result, there is a high probability that clay mineral structural formulas generated solely from XRD-bulk chemical analyses reflect the compositions of sample impurities. Furthermore, the common practice of assigning mineral names to expandable and nonexpandable layers of uncertain chemical composition strictly on the basis of XRD data contributes another dimension of uncertainty in assessing the mineralogy of clay mineral samples. For example, the expandability of a clay sample detected by XRD may be caused by interparticle diffraction rather than the presence of smectite (Nadeau *et al.*, 1984a, 1984b; Eberl *et al.*, 1987). Consequently, the actual compositional variation in smectite or illite is probably much more restricted than that inferred from most compilations of compositional data, such as that shown in Figure 1. This observation is supported by the analysis of compositional data summarized in the following pages, which is based on objective selection criteria designed to minimize the uncertainties adduced above.

A number of recent attempts to distinguish chemically between smectite and illite rely on coupling transmission electron microscopy (TEM) with analytical electron microanalysis (AEM) and/or other microchemical techniques to study single crystals of clay minerals (Ireland *et al.*, 1983; Duplay, 1984; Lee *et al.*, 1985; Ahn and Peacor, 1986; Yau *et al.*, 1987; Huff *et al.*, 1988; Warren and Curtis, 1989; Inoue *et al.*, 1987, 1990; Jiang *et al.*, 1990). However, studies of this kind have been performed only on samples from a limited number of sites and geologic environments. Although some trends in the compositions of smectite and illite have been identified from high resolution TEM studies, enough data of this kind are not yet available or sufficiently quantitative to resolve the compositional am-

https://doi.org/10.1346/CCMN.1993.0410503 Published online by Cambridge University Press

biguities represented by the overlapping fields in Figure 1. Consequently, most of what we know about the chemistry of smectite and illite comes from combined XRD and bulk chemical analyses of clay samples that are reported in the literature to consist solely of smectite or illite without confirmation by TEM or AEM studies. Combining these data with compositional trends identified by TEM/AEM and other bulk techniques such as Mössbauer spectroscopy and NMR facilitates critical analysis of smectite and illite compositions.

ANALYSIS OF COMPOSITIONAL DATA

As discussed by Aagaard and Helgeson (1983), derivation of the structural formulas of clay minerals from chemical analyses of bulk samples may result in compositional ambiguities arising from sample heterogeneity. However, such ambiguities can be minimized if objective selection criteria are established to discriminate among sample analyses in order to identify those most representative of smectite or illite. The following selection criteria were used in the present study to evaluate all of the sample analyses of smectite and illite that could be found in the literature over the past four decades. These were: 1) no sample impurities were detected by XRD, 2) the reported composition of the mineral in oxide weight percent sums to 97–102%, 3) analytical determinations were made independently for FeO and Fe_2O_3, 4) the illite samples contained $\leq 15\%$ expandable layers and/or had a cation exchange capacity (CEC) of ≤ 45 meq g^{-1}, and 5) the smectite samples contained $\geq 85\%$ expandable layers and/or had a CEC of ≥ 90 meq g^{-1}. Because interpretation of both CEC and measurements of sample expandability are subject to a host of uncertainties (Ransom and Helgeson, 1989), the last two criteria were established simply as gross, but not necessarily reliable, indicators of smectite or illite sample purity. The CEC and expandability criteria for smectite were set at high values to guarantee selection of samples composed primarily of sheet silicates with low layer charges. Less restrictive criteria were adopted for illite because CEC and sample expandability are affected by grain size. For example, TEM studies of illite samples show that many of them consist primarily of thin particles. These particles may increase CEC values to moderate levels as water or ethylene glycol molecules are adsorbed on the upper and lower free surfaces of the particles. As a result, sample expandability may occur even in the absence of smectite (Nadeau *et al.*, 1984a, 1984b, 1984c; Eberl *et al.*, 1987).

Structural formulas of smectite and illite written in terms of a half unit cell [i.e., $O_{10}(OH)_2$] that fit all of the selection criteria stipulated above were computed in the present study from reported oxide weight percents using the procedure described by Newman and Brown (1987, p. 15) after removing the weight percents of TiO_2 and MnO from the analyses; these were then normalized to 100%. The analyses of TiO_2 and MnO were excluded because Ross and Hendricks (1945), Schultz (1969), and Weaver and Pollard (1973) concluded that Ti^{4+} and Mn^{2+} in most chemical analyses of smectite and illite are caused by small amounts of cryptocrystalline rutile and manganese oxides that cannot be detected by XRD. This conclusion is supported by recent AEM analyses of smectite and illite that have been identified as such by careful TEM studies. No Ti or Mn is reported in these analyses, except for two illites analyzed by Warren and Curtis (1989), which contain only 0.02 atoms of Ti based on a structural formula for $O_{10}(OH)_2$.

Site occupancies in smectite and illite structural formulas computed from chemical analyses reported in the literature are listed in Tables 1 and 2. Although hundreds of analyses were considered, only those represented by the occupancies shown in these tables met the selection criteria described above. Despite the fact that the analyses in Tables 1 and 2 are small in number, they represent a wide range of geologic environments and lithologies. It can be deduced from these tables that both smectite and illite exhibit substantial variation in their 2:1 silicate layer compositions. It is also apparent that the negative layer charge is small (~0.3–0.5) in the smectite samples. This charge is generally satisfied in geologic systems by Na^+, Ca^{2+}, and K^+ on the interlayer sites in the mineral. In contrast, the layer charge in illite is more negative (~0.6–0.8) with interlayer sites that are nearly all occupied by K^+. The mole fraction of trivalent cations in the octahedral sites ($X_{R^{3+}}^{VI}$) of the smectites and illites represented by the analyses in Tables 1 and 2 are plotted in Figure 2 as a function of the mole fraction of Al in the tetrahedral sites (X_{Al}^{IV}). Smectite analyses are represented in this figure by circles and illite analyses by triangles. It can be seen that all but one of each type of symbol fall into separate groups in Figure 2. These groups are separated by a dashed vertical line at $X_{Al}^{IV} \cong 0.06$. Note that the symbols representing smectite and illite in Figure 2 are in adjacent fields, rather than being separated by a field of mixed-layered clays, such as that shown in a similar diagram generated by Aagaard and Helgeson (1983).

The difference in both the mole fraction of tetrahedral Al and the identity and concentration of the interlayer cations in the site occupancies shown in Tables 1 and 2 suggests that no continuous solid solution exists between smectite and illite. This conclusion is supported by site-charge correlations for smectite and illite (see below) as well as recent Mössbauer studies of these minerals (Heller-Kallai and Rozenson, 1981) and TEM/AEM studies of the chemistry and textural relations of illite and smectite clays in mineral separates and ion-milled thin sections (Ahn and Peacor, 1986; Yau *et al.*, 1987). The latter studies indicate that smectite reacts to form illite via a dissolution/precip-

https://doi.org/10.1346/CCMN.1993.0410503 Published online by Cambridge University Press

https://doi.org/10.1346/CCMN.1993.0410503 Published online by Cambridge University Press

Table 1. Illite site occupancies based on chemical formulas expressed in terms of a half unit cell [i.e., $O_{10}(OH)_2$] computed from chemical analyses taken from the literature.

K^+	Na^+	Ca^{2+}	NH_4^+	Mg^{2+}	Fe^{2+}	Al(VI)	Fe^{3+}	O_{OC}	Al(IV)	Si	CEC	%EXP	Sample provenance	Reference
0.69	0.03	0.05	0.00	0.36	0.07	1.55	0.04	2.02	0.43	3.57		<5	Marblehead, Fond Du Lac Co., Wisconsin	Gaudette (1965)
0.61	0.02	0.01	0.00	0.18	0.19	1.33	0.42	2.12	0.64	3.36		0	Beavers Bend, Broken Bow, Oklahoma	Gaudette *et al.* (1966)
0.58	0.03	0.03	0.00	0.20	0.08	1.65	0.07	2.00	0.41	3.59		~5	Rock Island, Rock Island Co., Illinois	Gaudette *et al.* (1966)
0.57	0.05	0.07	0.00	0.17	0.22	1.25	0.45	2.09	0.65	3.35		10 to 15	Frithian, Vermillion Co., Illinois	Gaudette *et al.* (1966)
0.73	0.01	0.02	0.00	0.28	0.01	1.67	0.04	2.00	0.47	3.53		6	Silurian, Welsh borderlands, UK, M11	Srodon *et al.* (1986)
0.68	0.01	0.04	0.00	0.35	0.02	1.53	0.11	2.00	0.41	3.59		7	Silurian, Welsh borderlands, UK, M8	Srodon *et al.* (1986)
0.58	0.01	0.07	0.00	0.30	0.02	1.54	0.16	2.02	0.46	3.54		13	Silurian, Welsh borderlands, UK, M7	Srodon *et al.* (1986)
0.56	0.01	0.05	0.00	0.40	0.02	1.56	0.05	2.03	0.33	3.67		15	Silurian, Welsh borderlands, UK, M4	Srodon *et al.* (1986)
0.71	0.01	0.03	0.00	0.29	0.08	0.97	0.70	2.04	0.53	3.47		<10	Morrison, Colorado	Hower and Mowatt (1966)
0.67	0.02	0.02	0.00	0.23	0.02	1.74	0.03	2.02	0.55	3.45		10	Steamboat Springs, Colorado	Hower and Mowatt (1966)
0.64	0.02	0.00	0.00	0.26	0.05	1.57	0.15	2.03	0.43	3.57	21	10	Clinton, New York	Hower and Mowatt (1966)
0.62	0.01	0.00	0.00	0.35	0.07	1.46	0.15	2.03	0.30	3.70	20	10	Eau Claire, Illinois Basin	Hower and Mowatt (1966)
0.58	0.01	0.00	0.00	0.30	0.03	1.55	0.14	2.01	0.31	3.69	24	15	New Albany, Indiana	Hower and Mowatt (1966)
0.57	0.01	0.01	0.00	0.38	0.01	1.44	0.16	2.00	0.20	3.80	25	15	Lowville, Fort Plain, New York	Hower and Mowatt (1966)
0.76	0.03	0.01	0.00	0.31	0.04	1.65	0.03	2.04	0.55	3.45	11	<10	Interlake, Williston Basin, Montana	Hower and Mowatt (1966)
0.69	0.01	0.00	0.00	0.31	0.08	1.35	0.27	2.01	0.36	3.64	13	<10	Silverhill, Jefferson Canyon, Montana	Hower and Mowatt (1966)
0.58	0.00	0.07	0.07	0.38	0.03	1.58	0.03	2.02	0.41	3.59	33		Kalkberg, New York	Nadeau and Bain (1986)
0.56	0.00	0.08	0.14	0.24	0.01	1.67	0.05	1.97	0.53	3.47	40		Tioga, New York	Nadeau and Bain (1986)
0.74	0.00	0.05	0.04	0.16	0.05	1.71	0.07	1.99	0.64	3.36		0	Rotligiend, North Sea	Nadeau and Bain (1986)

O_{OC} indicates the octahedral occupancy of the mineral, %EXP designates the percent expandable layers in the sample, CEC stands for the cation exchange capacity of the clay, Al(VI) represents octahedral aluminum, and Al(IV) denotes tetrahedral aluminum.

Table 2. Smectite site occupancies based on chemical formulas expressed in terms of a half unit cell [i.e., $O_{10}(OH)_2$] computed from chemical analyses taken from the literature.

K^+	Na^+	Ca^{2+}	Mg^{2+}	Fe^{2+}	Al(VI)	Fe^{3+}	O_{OC}	Al(IV)	Si	CEC	% EXP.	Sample provenance	Reference
0.05	0.39	0.05	0.41	0.00	1.51	0.07	1.99	0.10	3.90		95	Disturbed Belt, Montana, LT-42	Eslinger *et al.* (1979)
0.06	0.58	0.06	0.19	0.00	1.51	0.23	1.92	0.34	3.66		93	Disturbed Belt, Montana, LT-139A	Eslinger *et al.* (1979)
0.03	0.16	0.10	0.49	0.04	1.46	0.13	2.13	0.25	3.75	100		Gammano, Italy bentonite	Weaver and Pollard (1973)
0.00	0.39	0.00	0.39	0.01	1.26	0.37	2.03	0.07	3.93	107		Redhill, England montmorillonite	Weir (1965)
0.00	0.36	0.00	0.25	0.01	1.57	0.19	2.02	0.15	3.85	103		Wyoming montmorillonite	Weir (1965)
0.00	0.01	0.24	0.30	0.00	1.69	0.01	2.01	0.20	3.80	103		Greenwood, Maine	Foster (1953)
0.01	0.01	0.18	0.46	0.01	1.43	0.14	2.04	0.03	3.97	90		Burns	Foster (1953)
0.00	0.36	0.00	0.25	0.01	1.57	0.19	2.02	0.15	3.85	100		Wyoming	Schultz (1969)
0.05	0.03	0.19	0.53	0.02	1.43	0.08	2.06	0.07	3.93	124		Polkville, Mississippi	Kerr (1950)
0.00	0.18	0.02	0.32	0.01	1.58	0.15	2.06	0.06	3.94	102		Upton	Kerr (1950)
0.04	0.03	0.17	0.51	0.01	1.41	0.13	2.06	0.07	3.93	171		Burns	Kerr (1950)
0.03	0.02	0.19	0.40	0.02	1.48	0.13	2.03	0.10	3.90	159		Chambers	Kerr (1950)
0.03	0.02	0.11	0.32	0.02	1.54	0.20	2.08	0.16	3.84	127		Lorena	Kerr (1950)
0.48	0.00	0.00	0.50	0.01	1.37	0.14	2.02	0.03	3.97	110		Amargosa Valley, California	Foster (1951)
0.50	0.00	0.00	0.42	0.01	1.46	0.13	2.02	0.13	3.87	115		Hector, California	Foster (1951)
0.42	0.00	0.00	0.32	0.00	1.69	0.01	2.02	0.19	3.81	97		Pala, California	Foster (1951)
0.43	0.00	0.00	0.38	0.02	1.47	0.15	2.02	0.09	3.91	97		Ardmore, South Dakota	Foster (1951)

O_{OC} indicates the octahedral occupancy of the mineral, %EXP designates the percent expandable layers in the sample, CEC stands for the cation exchange capacity of the clay, Al(VI) represents octahedral aluminum, and Al(IV) denotes tetrahedral aluminum.

itation mechanism, rather than by exsolution or through coupled tetrahedral-interlayer substitutions that take place in the solid state. It thus appears that smectite and illite form separate solid solutions, each of which involves the substitution of Al for Si on the tetrahedral sites and/or divalent cations for trivalent cations on the octahedral sites. These substitutions, in turn, may be coupled to each other and/or the cation occupancy of the interlayer sites. Furthermore, evidence adduced below indicates that limited solid solubility may occur between dioctahedral and trioctahedral components in both smectite and illite solid solutions.

Site-charge correlations and compositional end members

Structural considerations (Newman and Brown, 1987) and thermodynamic analysis of aqueous solution compositions coexisting with smectites and illites in natural systems (Garrels, 1984) suggest that the number of cations occupying the octahedral sites of illites and smectites ranges from ~1.9–2.1 [per $O_{10}(OH)_2$]. The site occupancies in Tables 1 and 2 support this conclusion. The extent of the variation in octahedral site occupancy (O_{OC}) in these minerals can be assessed in Figure 3, where the octahedral occupancies of the illites and smectites given in Tables 1 and 2 are indicated by black bars. It can be seen in this figure that octahedral site occupancies in smectite vary from ~1.9–2.13 and those in illite from ~1.95–2.11. It can also be seen that the distribution of O_{OC} for both minerals is skewed to values greater than 2.0. Although total octahedral site occupancies that differ from 2.0 [per $O_{10}(OH)_2$] by more than $\sim\pm0.05$ are generally taken to indicate the presence of undetected cryptocrystalline impurities in the clay samples (Weaver and Pollard, 1973; Newman and Brown, 1987), octahedral occupancies slightly greater or less than 2.0 may also result from limited dioctahedral-trioctahedral and dioctahedral-vacancy solid solution (Kelley, 1945). Because the samples represented by the site occupancies shown in Tables 1 and 2 meet the selection criteria described above, the variation of O_{OC} in the tables can be attributed to solid solution. Taking account of the spread of octahedral occupancies shown in Figure 3, it seems reasonable to assume limits of total octahedral site occupancy of 2.0 ± 0.1 for both smectite and illite. A search of the literature reveals that other dioctahedral 2:1 layer silicates such as coarsely crystalline muscovite exhibit a similar spread in octahedral occupancy. This similarity in the octahedral occupancies of large flakes of muscovite and fine-grained clay samples suggests that limited dioctahedral-trioctahedral and dioctahedral-vacancy solid solution in illite, smectite, and other layer silicates is commonplace.[4]

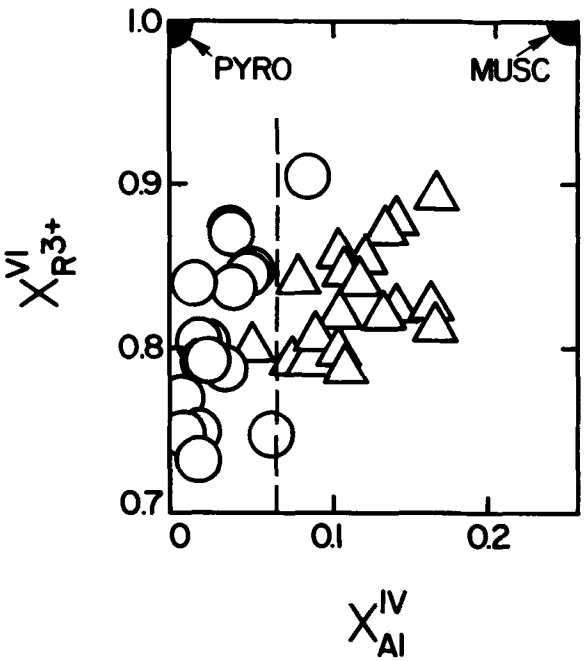


Figure 2. Mole fractions of trivalent cations in the octahedral sites (X^{VI}_{R3+}) of the smectites (circles) and illites (triangles) represented by the site occupancies given in Tables 1 and 2, as a function of the mole fraction of tetrahedral Al (X^{IV}_{Al}) in the minerals. The dashed vertical line at $X^{IV}_{Al} = 0.06$ represents the approximate maximum and minimum values of tetrahedral substitution in smectites and illites, respectively. Values of X^{VI}_{R3+} and X^{IV}_{Al} corresponding to those for stoichiometric pyrophyllite (PYRO) and muscovite (MUSC) are indicated in the upper corners of the diagram. The size of the symbols corresponds to the minimum uncertainty in the amount of tetrahedral Al or octahedral R^{3+} calculated for each structural formula (Warren and Ransom, 1992).

Because demonstrable variation occurs in the octahedral occupancy of smectites and illites, four descriptive generic variables are required to describe the compositions of these minerals: one accounting for the total number of octahedrally coordinated cations (O_{OC}), and three others representing the total cation charge on the interlayer (Z_I), octahedral (Z_O), and tetrahedral (Z_T) sites. These quantities are given in Tables 3 and 4 for the site occupancies listed in Tables 1 and 2, respectively. It should be noted that only two of the three charge variables shown in Tables 3 and 4 are independent of one another, owing to the requirement that electrical neutrality be maintained (see below).

Illite solid solutions. The tetrahedral, octahedral, and interlayer cation charges for illites shown in Table 3 are plotted against each other in Figures 4–6. As discussed by Warren and Ransom (1992), site occupancies

[4] It has been shown that muscovite flakes that appear from XRD diffractograms or petrographic analysis to be pure may, in fact, contain small inclusions of other minerals. However, the volume of these inclusions and their contribution to the bulk chemistry and stoichiometry of the mineral are generally negligible (Page, 1980).

https://doi.org/10.1346/CCMN.1993.0410503 Published online by Cambridge University Press

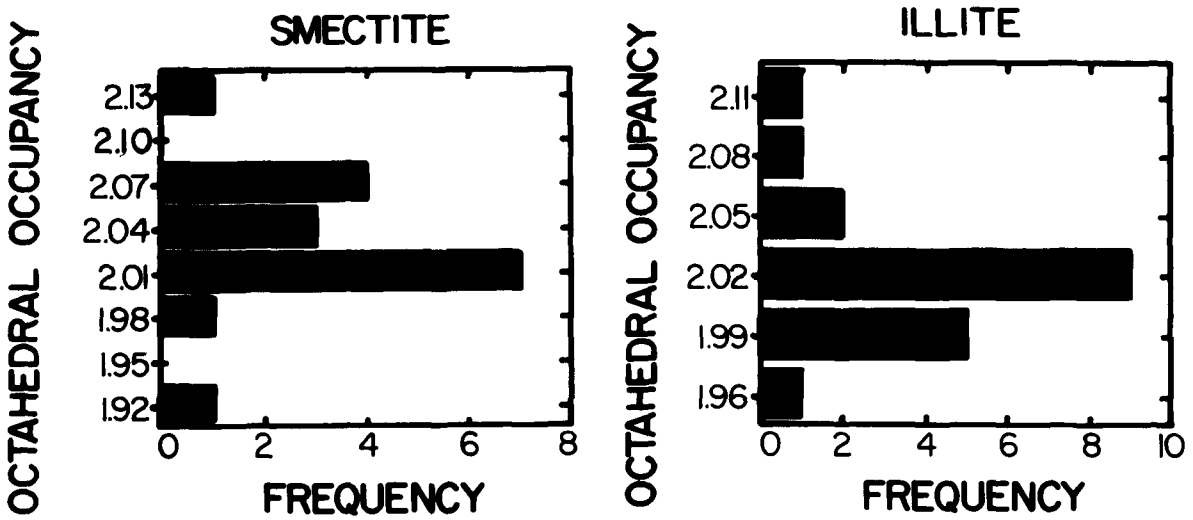


Figure 3. Histograms representing the octahedral occupancies (O_{OC}) of the smectites and illites given in Tables 3 and 4. Each bar represents the number of smectite or illite analyses that fall within the range defined by the labeled $O_{OC} \pm 0.01$.

specified in most clay mineral structural formulas derived from XRD-bulk chemical data are at best significant to the first decimal place. The size of the circles plotted in Figures 4–6 represents this minimum uncertainty (i.e., ±0.05). The white and gray symbols shown in these figures denote $O_{OC} > 2.03$ and $O_{OC} = 2.0 \pm 0.03$, respectively. Hence, the circles designate values of O_{OC} that fall either above, on, or below the plane of the paper, which represents $O_{OC} = 2.0$. It can be seen in Figure 4 that the tetrahedral cation charge in illites correlates well with the interlayer cation charge. For most natural illites, this coincides with the number of K^+ cations in the interlayer sites. A similar but less pronounced correlation of tetrahedral and octahedral charge is apparent in Figure 5. Straight lines were drawn through the gray symbols in Figures 4 and 5 representing the data for which $O_{OC} = 2.0 \pm 0.03$. It is apparent in these figures that the lines intersect most of the gray circles and that their centers fall within 0.1 charge units of the lines. The latter difference is well within the analytical uncertainties of the data represented by the symbols. The straight lines drawn in Figures 4 and 5 are consistent with electrical neutrality, which requires

$$Z_T + Z_O + Z_I = 22 \quad (1)$$

where 22 denotes the negative layer charge of the min-

Table 3. Octahedral occupancy (O_{OC}) and site charges on the interlayer (Z_I), octahedral (Z_O), and tetrahedral (Z_T) sites in the illite solid solutions represented by the site occupancies shown in Table 1.

O_{OC}	Z_I	Z_O	Z_T
1.99	0.55	5.56	15.90
1.92	0.76	5.58	15.66
2.13	0.39	5.86	15.75
2.03	0.39	5.68	15.92
2.02	0.37	5.79	15.85
2.01	0.49	5.71	15.80
2.04	0.39	5.64	15.97
2.02	0.37	5.79	15.85
2.06	0.44	5.63	15.93
2.06	0.21	5.85	15.94
2.06	0.41	5.65	15.93
2.03	0.44	5.67	15.90
2.08	0.26	5.90	15.84
2.02	0.48	5.55	15.97
2.02	0.50	5.63	15.87
2.02	0.42	5.74	15.81
2.02	0.43	5.66	15.91

Table 4. Octahedral occupancy (O_{OC}) and site charges on the interlayer (Z_I), octahedral (Z_O), and tetrahedral (Z_T) sites in the smectite solid solutions represented by the site occupancies shown in Table 2.

O_{OC}	Z_I	Z_O	Z_T
2.02	0.82	5.62	15.57
2.12	0.66	5.98	15.36
2.00	0.68	5.73	15.59
2.09	0.76	5.89	15.35
2.00	0.77	5.70	15.53
2.00	0.78	5.64	15.59
2.02	0.73	5.73	15.54
2.03	0.67	5.66	15.67
2.04	0.78	5.75	15.47
2.02	0.73	5.82	15.45
2.03	0.66	5.77	15.57
2.03	0.64	5.66	15.70
2.01	0.59	5.72	15.69
2.00	0.60	5.60	15.80
2.04	0.79	5.76	15.45
2.01	0.70	5.65	15.64
2.02	0.79	5.65	15.59
1.97	0.86	5.66	15.47
1.99	0.88	5.76	15.36

https://doi.org/10.1346/CCMN.1993.0410503 Published online by Cambridge University Press

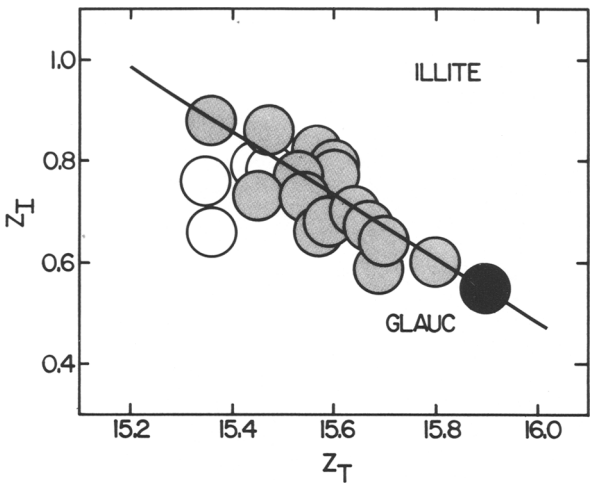


Figure 4. Interlayer charge (Z_I) in illite plotted as a function of the tetrahedral charge (Z_T) for the site charges given in Table 3. The white and gray circles represent stoichiometries for which $O_{OC} < 2.03$ and $O_{OC} = 2.0 \pm 0.03$, respectively. The black circle denotes a glauconitic compositional end member designated for the purposes of this communication as GLAUC (see text). The straight line drawn through the symbols represents data for which $O_{OC} = 2.0 \pm 0.03$.

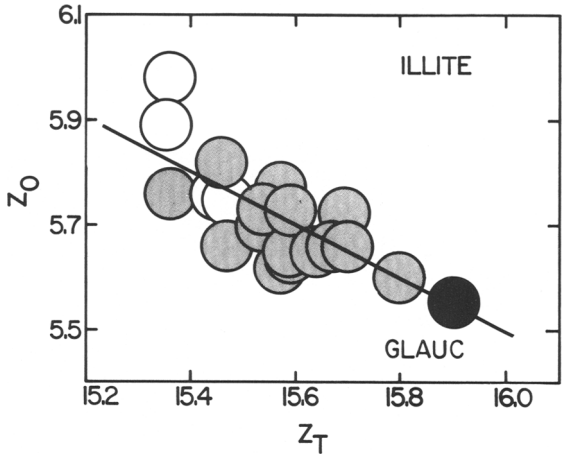


Figure 5. Octahedral charge (Z_O) in illite plotted as a function of the tetrahedral charge (Z_T) for the site charges given in Table 3 (see text and caption of Figure 4).

eral per $O_{10}(OH)_2$. As a consequence, the slope and intercept of the straight line in Figure 6 are determined by those in Figures 4 and 5. Although the symbols in Figures 5 and 6 are clustered over small intervals of Z_O, it can be seen that the line in this figure is nevertheless consistent with the distribution of the bulk of the symbols. Inspection of the data shown in Figures 4–6 indicates that the bulk of the cation charge in the interlayer sites in illites is compensated predominantly by the cation charge-deficiency in the tetrahedral sites of the mineral. Despite the fact that the symbols in Figures 4–6 are somewhat scattered, they are for the most part consistent with limited trioctahedral-dioctahedral and dioctahedral-vacancy solid solution.

Following Holdaway (1980), the term compositional end member is used in the present communication to refer to a nonstoichiometric limit of compositional variation exhibited by a solid solution.[5] As such, the compositions of these end members are arbitrary, provided they fulfill the criteria that they bracket the range of compositional variation in the mineral. In the case of the illites considered in the present study, an adequate set of compositional end members must not only satisfy the trends shown in Figures 4–6, but must also bracket total octahedral occupancies (O_{OC}) from 1.9–2.1 (see above). The lines in Figures 4–6 permit a generalized compositional end member to be selected for illite solid solutions with $O_{OC} = 2.0$. This generalized composition is indicated by the black GLAUC circles in Figures 4–6, which represents the formula unit

$$A_{0.55}R^{2+}_{0.45}R^{3+}_{1.55}Al_{0.1}Si_{3.9}O_{10}(OH)_2 \qquad (2)$$

where A denotes a monovalent cation or its divalent charge equivalent (e.g., $Ca^{2+}/2$), and R^{2+} and R^{3+} stand for divalent and trivalent cations, respectively.

It has been shown by Garrels (1984) that illites in equilibrium with natural waters can be described in terms of an end member with an octahedral occupancy of 1.9 (AL-ILL) and a generalized chemical formula corresponding to

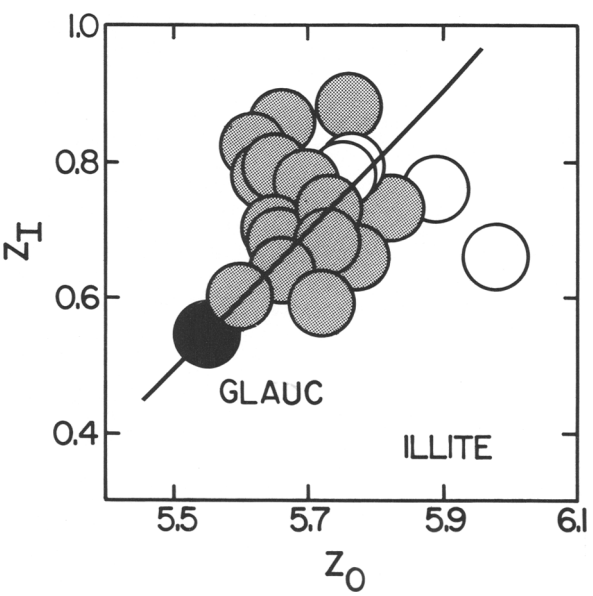


Figure 6. Interlayer charge (Z_I) in illite plotted as a function of the octahedral charge (Z_O) for the site charges given in Table 3 (see text and caption of Figure 4).

[5] For example, the end-member formula for chlorite in pelitic rocks saturated with Al and Si corresponds to $Fe_{4.54}Al_{2.92}Si_{2.54}O_{10}(OH)_8$ (Holdaway, 1980).

https://doi.org/10.1346/CCMN.1993.0410503 Published online by Cambridge University Press

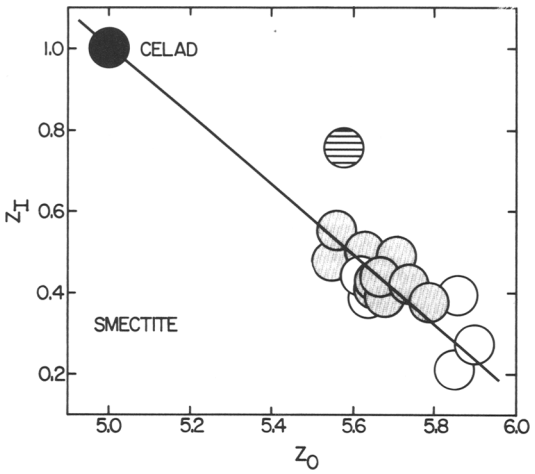


Figure 7. Interlayer charge (Z_I) in smectite plotted as a function of the octahedral charge (Z_O) for the site charges given in Table 4. The gray and white circles represent stoichiometries for $O_{OC} > 2.0 \pm 0.03$ and $O_{OC} < 2.03$, respectively. The striped circle denotes $O_{OC} < 1.97$ and the black circle designates stoichiometric celadonite. The straight line drawn through the symbols represents $O_{OC} = 2.0 \pm 0.03$ (see text).

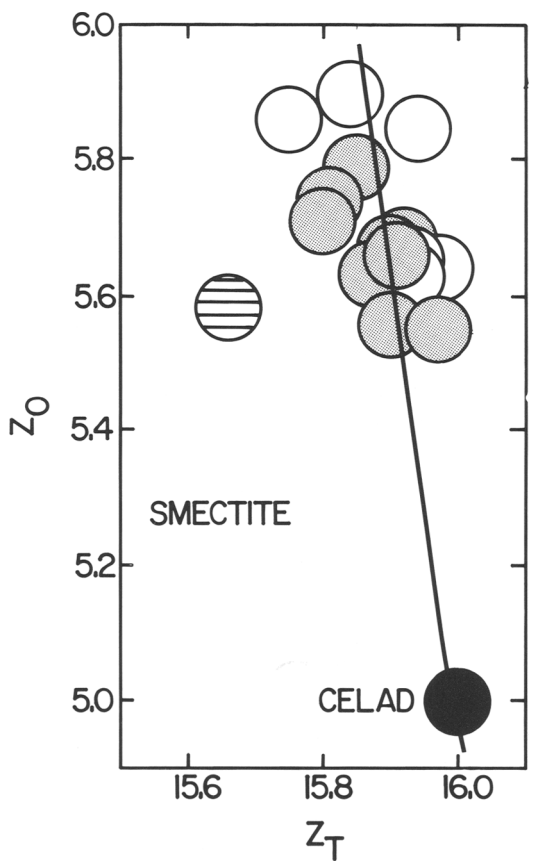


Figure 8. Octahedral charge (Z_O) in smectite plotted as a function of the tetrahedral charge (Z_T) for the site charges given in Table 4 (see text and caption of Figure 7).

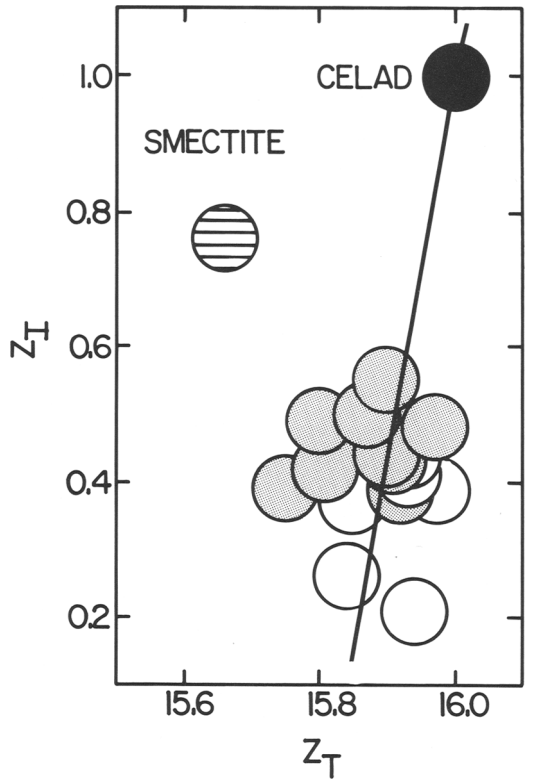


Figure 9. Octahedral charge (Z_I) in smectite plotted as a function of the tetrahedral charge (Z_T) for the site charges given in Table 4 (see text and caption of Figure 7).

$$A_{0.8}R^{3+}_{1.9}Al_{0.5}Si_{3.5}O_{10}(OH)_2. \quad (3)$$

This formula unit was selected in the present study as the illite solid solution end member for $O_{OC} = 1.9$. End member (3) and the equations of the lines shown in Figures 4–6 for $O_{OC} = 2.0$ determine the composition of a third generalized solid solution end member (MG-ILL) for which $O_{OC} = 2.1$. The generalized chemical formula of this end member is shown in Table 5, together with those of end members (2) and (3). These three end members form a compositional plane that is representative of the compositions of the bulk of the illite solid solutions represented by the site occupancies shown in Table 1. The equation of this plane is given by

$$565.5 = 4.5\ Z_O + 30.0\ Z_T + 31.5\ O_{OC}. \quad (4)$$

Eq. 4 is closely consistent with the compositional data shown in Table 1.

Smectite solid solutions. Diagrams similar to those described above for illite are depicted in Figures 7–9 for the smectite site occupancies shown in Table 2. Although no interlayer H_2O appears in this table, the compositional consequences of interlayer hydration are taken into account below. The diagrams shown in Figures 7–9 were generated using the values of Z_I, Z_T, and

https://doi.org/10.1346/CCMN.1993.0410503 Published online by Cambridge University Press

Z_O given in Table 4. The gray, striped, and white circles shown in these figures represent $O_{OC} = 2.0 \pm 0.03$, $O_{OC} < 1.97$, and $O_{OC} > 2.03$, respectively. As expected, there is a correlation in Figure 7 between the cation charge on the octahedral and interlayer sites of smectite. A similar but less pronounced correlation is apparent in Figure 8 between the cation charges in the octahedral and tetrahedral sites in the mineral.

Straight lines were drawn through the gray symbols in Figures 7 and 8 representing the data for which $O_{OC} = 2.0 \pm 0.03$. It can be seen in these figures that the lines are within 0.1 charge units of the centers of the gray circles, which is well within the analytical uncertainty of the data represented by the symbols. As in Figures 4 and 5, the lines shown in Figures 7 and 8 are consistent with electrical neutrality (Eq. 1), which constrains the position and slope of the line in Figure 9. Although the symbols in Figure 9 are clustered over short intervals of Z_T, it can be seen that line 15 is consistent with most of the data represented by the symbols. It is apparent in Figures 7–9 that the bulk of the octahedral deficiency in smectite is compensated by the total charge of the cations in the interlayer sites. The data shown in these figures are generally consistent with limited trioctahedral-dioctahedral and dioctahedral-vacancy solid solution.

The lines drawn through the circles in Figures 7–9 representing $O_{OC} = 2.0$ intersect the generalized composition of stoichiometric celadonite (CELAD), which is represented by

$$AR^{2+}R^{3+}Si_4O_{10}(OH)_2 \quad (5)$$

where A denotes a monovalent cation or its divalent charge equivalent and R^{2+} and R^{3+} stand for divalent and trivalent cations, respectively. Celadonite is thus a compositional end member of smectite solid solutions for which the octahedral occupancy is 2.0. As in the case of illite, the smectite end member adopted in the present study to represent $O_{OC} = 1.9$ (AL-SMEC) corresponds to the smectite end member proposed by Garrels (1984). This end member was selected because it is consistent with water compositions reported to be in equilibrium with smectites in natural systems (Aagaard and Helgeson, 1983; Garrels, 1984). The generalized chemical formula of the end member is

$$A_{0.3}Al_{1.9}Si_4O_{10}(OH)_2. \quad (6)$$

Taking account of the compositions of smectite solid solution end members (5) and (6), together with the equations of the lines shown in Figures 7–9 for $O_{OC} = 2.0$, the site occupancy in a third smectite solid solution generalized end member (MG-SMEC) can be calculated for $O_{OC} = 2.1$. The result of this calculation is shown in Table 5, together with the chemical formulas of the other two smectite solid solution end members. As in the case of illite solid solutions, these three end members form a compositional plane which is representative of the compositions of the bulk of the smectite solid solutions with the site occupancies shown in Table 2. The equation of this plane is

$$25.0 = 2.0\ Z_O + Z_T - O_{OC}, \quad (7)$$

which represents closely the bulk of the compositional data for smectite solid solutions in Table 2.

Table 5. Generalized compositional end members of the illite and smectite solid solutions represented by the site occupancies shown in Tables 1 and 2.

Smectite solid solutions	
AL-SMEC	$A_{0.3}R^{3+}_{1.9}Si_4O_{10}(OH)_2$
MG-SMEC	$A_{0.25}R^{2+}_{0.3}R^{3+}_{1.8}Al_{0.25}Si_{3.75}O_{10}(OH)_2$
CELAD	$AR^{2+}R^{3+}Si_4O_{10}(OH)_2$
Illite solid solutions	
AL-ILL	$A_{0.8}R^{3+}_{1.9}Al_{0.5}Si_{3.5}O_{10}(OH)_2$
MG-ILL	$A_{0.9}R^{2+}_{0.3}R^{3+}_{1.8}Al_{0.9}Si_{3.1}O_{10}(OH)_2$
GLAUC	$A_{0.55}R^{2+}_{0.45}R^{3+}_{1.55}Al_{0.1}Si_{3.9}O_{10}(OH)_2$

A represents monovalent cations or divalent cations expressed in terms of their monovalent equivalent (e.g., $Ca^{2+}/2$), R^{2+} stands for the divalent cations Mg^{2+} and Fe^{2+}, and R^{3+} refers to the trivalent cations Al^{3+} and Fe^{3+}.

THERMODYNAMIC COMPONENTS

The term thermodynamic component is used in the present communication in its strict sense. A thermodynamic component of a mineral corresponds to a chemical formula unit representing one of the minimum number of independent variables required to describe the composition of the mineral. Any set of thermodynamic components can be chosen for this purpose, none of which is uniquely suitable. However, one set may be more convenient to use in a particular context than another. A thermodynamic component need have no physical significance and (assertions to the contrary by Lippmann, 1977 and 1982, notwithstanding) the chemical formula representing a thermodynamic component does not necessarily have to conform to both the law of definite proportions and the concept of a unit cell, provided that it satisfies the requirement that it is one of a minimum number of independent compositional variables in the system. As such, it can be either added to, or subtracted from a system to describe the composition of a phase. Unlike solid solutions, stoichiometric minerals consist of only one component with a chemical formula corresponding to that of the mineral. In the case of smectite and illite solid solutions, thermodynamic components corresponding to phyllosilicate species for which the thermodynamic properties are known facilitate calculation of the relative stabilities or metastabilities of illite and smectite solid solutions in geologic systems.

The compositions of each set of the three nonstoichiometric end members of illite and smectite solid solutions shown in Table 5 can be expressed in terms of four generic thermodynamic components. These are

https://doi.org/10.1346/CCMN.1993.0410503 Published online by Cambridge University Press

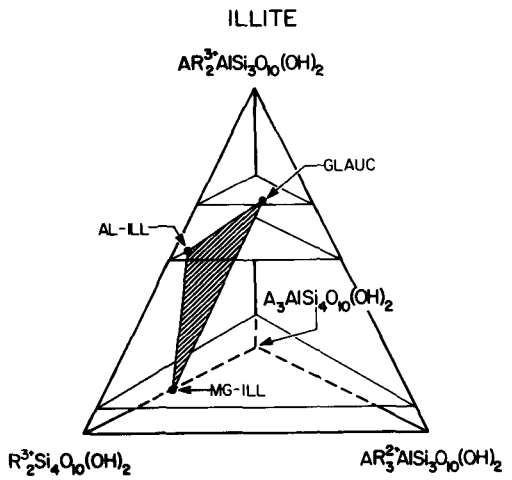


Figure 10. Generalized composition diagram for the generic system $AR_2^{3+}AlSi_3O_{10}(OH)_2$–$R_2^{3+}Si_4O_{10}(OH)_2$-$A_3AlSi_4O_{10}(OH)_2$$AR_3^{2+}AlSi_3O_{10}(OH)_2$ (see text).

$AR_2^{3+}AlSi_3O_{10}(OH)_2$, $R_2^{3+}Si_4O_{10}(OH)_2$, $A_3AlSi_4O_{10}(OH)_2$, and $R_2^{3+}Si_4O_{10}(OH)_2$, for smectite solid solutions and $AR_2^{3+}AlSi_3O_{10}(OH)_2$, $AR_3^{2+}AlSi_3O_{10}(OH)_2$, $R_2^{3+}Si_4O_{10}(OH)_2$, and $A_3AlSi_4O_{10}(OH)_2$ for illite solid solutions. The representative compositional planes described by Eqs. 4 and 7 are depicted in Figures 10 and 11, respectively, in terms of these two sets of generic thermodynamic components, which correspond to the apices of the compositional tetrahedrons shown in the figures. The end members of the two solid solutions plot on the horizontal reference planes in these tetrahedrons. It can be deduced from Figures 10 and 11 that the two tetrahedrons share a common face corresponding to the subsystem $R_2^{3+}Si_4O_{10}(OH)_2$–$AR_2^{3+}AlSi_3O_{10}(OH)_2$–$A_3AlSi_4O_{10}(OH)_2$. It follows that the two tetrahedrons can be combined to form the trigonal bipyramid shown in Figure 12. The end members of the smectite and illite solid solutions plot in Figure 12 on the planes circumscribed by the dashed and dotted lines, respectively. It can be seen in this figure that the representative compositional planes for the illite and smectite solid solutions (shown as dark planes) each have one compositional end member that falls on the horizontal plane of symmetry in the trigonal bipyramid. Nevertheless, the orientations of the dark planes are completely different, *which precludes mutual solid solubility between smectite and illite solid solutions.*

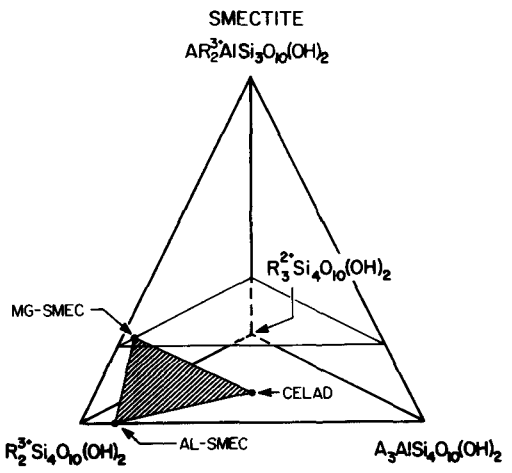


Figure 11. Generalized composition diagram for the generic system $AR_2^{3+}AlSi_3O_{10}(OH)_2$-$R_2^{3+}Si_4O_{10}(OH)_2$-$A_3AlSi_4O_{10}(OH)_2$-$AR_3^{2+}$-$Si_4O_{10}(OH)_2$ (see text).

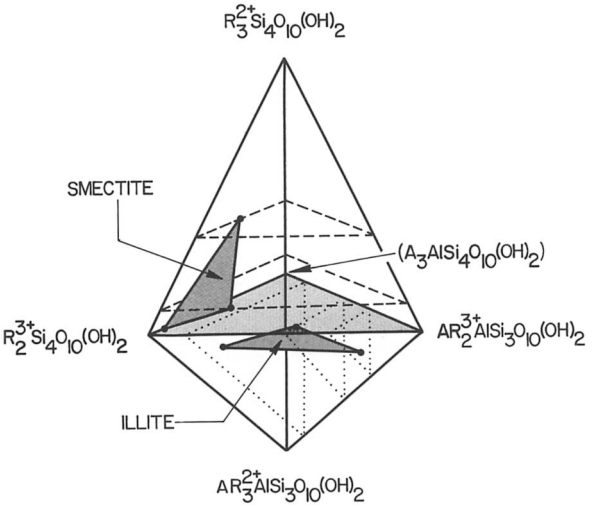


Figure 12. Illustration of the relative positions of the smectite and illite compositional planes with respect to one another in a trigonal dipyramid representing the overall generic system, $R_2^{3+}Si_4O_{10}(OH)_2$–$R_2^{3+}Si_4O_{10}(OH)_2$–$A_3AlSi_4O_{10}(OH)_2$–$AR_2^{3+}AlSi_3O_{10}(OH)_2$–$AR_3^{2+}AlSi_3O_{10}(OH)_2$. The upper and lower pyramids correspond to the compositional tetrahedrons for illite and smectite in Figures 10 and 11, respectively (see text).

The generic thermodynamic components that appear at the apices of the tetrahedrons depicted in Figures 10 and 11 can be recast in terms of actual thermodynamic components by taking account of the site occupancies in natural smectites and illites shown in Tables 1 and 2. Sets of these components for illite and dioctahedral aluminous smectite solid solutions are given in Table 6. Although nine of the twelve different

Table 6. Thermodynamic components of smectite and illite solid solutions for a half unit cell $[O_{10}(OH)_2]$.

	Smectite		Illite
1	$NaAl_3Si_3O_{10}(OH)_2 \cdot 4.5H_2O$	1	$KMg_3AlSi_3O_{10}(OH)_2$
2	$NaAl_3Si_3O_{10}(OH)_2$	2	$KFe_3AlSi_3O_{10}(OH)_2$
3	$Ca_{0.5}Al_3Si_3O_{10}(OH)_2$	3	$KFe_2AlSi_3O_{10}(OH)_2$
4	$KAl_3Si_3O_{10}(OH)_2$	4	$KAl_3Si_3O_{10}(OH)_2$
5	$K_3AlSi_4O_{10}(OH)_2$	5	$K_3AlSi_4O_{10}(OH)_2$
6	$Mg_3Si_4O_{10}(OH)_2$	6	$Al_2Si_4O_{10}(OH)_2$
7	$Fe_3Si_4O_{10}(OH)_2$		
8	$Fe_2Si_4O_{10}(OH)_2$		
9	$Al_2Si_4O_{10}(OH)_2$		

https://doi.org/10.1346/CCMN.1993.0410503 Published online by Cambridge University Press

thermodynamic components shown in Table 6 correspond in composition to stoichiometric minerals, the remaining three [$K_3AlSi_4O_{10}(OH)_2$, $Ca_{0.5}Al_3Si_3O_{10}(OH)_2$, and $NaAl_3Si_3O_{10}(OH)_2 \cdot 4.5H_2O$] are fictive. The component with the stoichiometry, $NaAl_3Si_3O_{10}(OH)_2 \cdot 4.5H_2O$, is included in Table 6 to provide explicitly for the contribution of interlayer H_2O to the compositions of smectite solid solutions. The chemical formula of this component is consistent with both vapor pressure isotherm data for smectites reported in the literature and a regular solution model of interlayer hydration in smectite solid solutions (Ransom and Helgeson, 1993b).

It can be seen in Table 6 that smectite solid solutions require nine thermodynamic components to account for the observed compositional and O_{OC} variation in this mineral. Because the illite solid solutions represented by the site occupancies shown in Table 1 contain no interlayer H_2O and so little Na^+, Ca^{2+}, and NH_4^+ compared with K^+ in the interlayer sites of the mineral, for practical purposes only the six thermodynamic components shown for the illite solid solutions in Table 6 are required to describe the compositions of these minerals. Note that nine oxide formula units (K_2O, Na_2O, CaO, MgO, FeO, Fe_2O_3, Al_2O_3, SiO_2, H_2O) are required to describe the compositions of the smectite solid solutions in Table 2, which corresponds to the number of thermodynamic components for these solid solutions in Table 6. In contrast, seven such units (K_2O, MgO, FeO, Fe_2O_3, Al_2O_3, SiO_2, H_2O) are needed to account for the compositions of the illite solid solutions in Table 1. Because the latter number exceeds that of the thermodynamic components for illite solid solutions in Table 6, this set of seven oxide chemical formula units does not constitute a valid set of thermodynamic components of illite solid solutions. It is of interest to note in this regard that the end members in Table 5 that appear at the apices of the dark planes in Figure 12 are valid thermodynamic components of any solid solutions with compositions that coincide with the planes.

In order to represent the structural formulas of natural smectites and illites in terms of the thermodynamic components given in Table 6, appropriate mole fractions of the components must be added to and subtracted from one another. Strategies for describing illite and smectite solid solution compositions and site occupancies in terms of the thermodynamic components in Table 6 are given below, together with the mole fractions of the components in both hypothetical smectite and illite solid solutions. In the following discussion, the lower case Greek letter ν is used to indicate the number of moles of a given subscripted species in one mole of either a smectite (s) or illite (i) solid solution, respectively, or a specific thermodynamic component (as for example in $\nu_{Na,s}$ and $\nu_{Na,NaAl_3Si_3O_{10}(OH)_2}$). The mole fractions of the components in both smectite and illite solid solutions are designated, for example, as $X_{NaAl_3Si_3O_{10}(OH)_2}$.

Smectite solid solutions

For example, $(Na_{0.22}Ca_{0.03}K_{0.01})(Mg_{0.29}Fe^{2+}_{0.03}Fe^{3+}_{0.12}Al_{1.66})(Al_{0.27}Si_{3.73})O_{10}(OH_2) \cdot 2.2H_2O$:

1. Compute the mole fraction of $NaAl_3Si_3O_{10}(OH_2) \cdot 4.5H_2O$ needed to account for the number of moles of interlayer H_2O in the chemical formula representing a half unit cell of the smectite solid solution ($\nu_{H_2O,s}$). If the amount of interlayer H_2O in the mineral is not reported, it can be estimated from equations and data given by Ransom and Helgeson (1993a, 1993b). In the case of the above smectite formula,

$$X_{NaAl_3Si_3O_{10}(OH)_2 \cdot 4.5\ H_2O} = \frac{\nu_{H_2O,s}}{\nu_{H_2O,NaAl_3Si_3O_{10}(OH)_2 \cdot 4.5\ H_2O}} = \frac{2.2}{4.5} = 0.489. \quad (8)$$

2. Assess $X_{NaAl_3Si_3O_{10}(OH)_2}$ from

$$X_{NaAl_3Si_3O_{10}(OH)_2} = \nu_{Na,s} - [(\nu_{Na,NaAl_3Si_3O_{10}(OH)_2 \cdot 4.5\ H_2O}) \cdot X_{NaAl_3Si_3O_{10}(OH)_2 \cdot 4.5\ H_2O}] \div (\nu_{Na,NaAl_3Si_3O_{10}(OH)_2}) = 0.22 - 0.489 = -0.269. \quad (9)$$

3. Calculate $X_{Ca_{0.5}Al_3Si_3O_{10}(OH)_2}$ from

$$X_{Ca_{0.5}Al_3Si_3O_{10}(OH)_2} = \frac{\nu_{Ca,s}}{\nu_{Ca,Ca_{0.5}Al_3Si_3O_{10}(OH)_2}} = \frac{0.03}{0.5} = 0.06. \quad (10)$$

4. Compute $X_{KAl_3Si_3O_{10}(OH)_2}$ from

$$X_{KAl_3Si_3O_{10}(OH)_2} = \frac{\nu_{Al^{IV},s} - \sum_{j=1}^{3}(4 - \nu_{Si,j})X_j}{4 - \nu_{Si,KAl_3Si_3O_{10}(OH)_2}} = 0.27 - 0.489 + 0.269 - 0.06 = -0.01 \quad (11)$$

where Al^{IV} stands for tetrahedral Al and the index j refers to the numbers of the smectite components ($j = 1, 2, \ldots$) in Table 6.

5. Assess $X_{K_3AlSi_4O_{10}(OH)_2}$ from

$$X_{K_3AlSi_4O_{10}(OH)_2} = \frac{\nu_{K,s} - (\nu_{K,KAl_3Si_3O_{10}(OH)_2})X_{KAl_3Si_3O_{10}(OH)_2}}{\nu_{K,K_3AlSi_4O_{10}(OH)_2}} = \frac{0.01 + 0.01}{3} = 0.0067. \quad (12)$$

https://doi.org/10.1346/CCMN.1993.0410503 Published online by Cambridge University Press

6. Evaluate:

$$X_{Mg_3Si_4O_{10}(OH)_2} = \frac{\nu_{Mg,s}}{\nu_{Mg,Mg_3Si_4O_{10}(OH)_2}} = \frac{0.29}{3} = 0.0967. \quad (13)$$

7. Compute $X_{Fe_3Si_4O_{10}(OH)_2}$ from

$$X_{Fe_3Si_4O_{10}(OH)_2} = \frac{\nu_{Fe^{2+},s}}{\nu_{Fe^{2+},Fe_3Si_4O_{10}(OH)_2}} = \frac{0.03}{3} = 0.01. \quad (14)$$

8. Solve:

$$X_{Fe_2Si_4O_{10}(OH)_2} = \frac{\nu_{Fe^{3+},s}}{\nu_{Fe^{3+},Fe_2Si_4O_{10}(OH)_2}} = \frac{0.12}{2} = 0.06. \quad (15)$$

9. Calculate $X_{Al_2Si_4O_{10}(OH)_2}$ from

$$X_{Al_2Si_4O_{10}(OH)_2} = \frac{\nu_{Si,s} - \sum_{j=1}^{8} \nu_{Si,j}X_j}{4}$$

$$= \frac{3.73 - 3(0.489) + 3(0.269) - 3(0.06) + 3(0.01)}{4} - \frac{4(0.0067) + 4(0.0967) + 4(0.01) + 4(0.06)}{4}$$

$$= 0.5567. \quad (16)$$

Illite solid solutions

For example, $K_{0.76}(Mg_{0.26}Fe^{2+}_{0.02}Fe^{3+}_{0.09}Al_{1.66})(Al_{0.57}Si_{3.43})O_{10}(OH)_2$:

1. Compute:

$$X_{KMg_3AlSi_3O_{10}(OH)_2} = \frac{\nu_{Mg,i}}{\nu_{Mg,KMg_3AlSi_3O_{10}(OH)_2}} = \frac{0.26}{3} = 0.867. \quad (17)$$

2. Evaluate:

$$X_{KFe_3AlSi_3O_{10}(OH)_2} = \frac{\nu_{Fe^{2+},i}}{\nu_{Fe^{2+},KFe_3AlSi_3O_{10}(OH)_2}} = \frac{0.02}{3} = 0.0067. \quad (18)$$

3. Solve:

$$X_{KFe_2AlSi_3O_{10}(OH)_2} = \frac{\nu_{Fe^{3+},i}}{\nu_{Fe^{3+},KFe_2AlSi_3O_{10}(OH)_2}} = \frac{0.09}{2} = 0.045. \quad (19)$$

4. Assess $X_{KAl_3Si_3O_{10}(OH)_2}$ from

$$X_{KAl_3Si_3O_{10}(OH)_2} = \frac{\nu_{Al^{IV},i} - \sum_{l=1}^{3}(4 - \nu_{Si,l})X_l}{4 - \nu_{Si,KAl_3Si_3O_{10}(OH)_2}}$$

$$= 0.57 - 0.0867 - 0.0067 - 0.045 = 0.4316. \quad (20)$$

where the index l refers to the numbers of the illite components (l = 1, 2, . . .) in Table 6.

5. Compute $X_{K_3AlSi_4O_{10}(OH)_2}$ from

$$X_{K_3AlSi_4O_{10}(OH)_2} = \frac{\nu_{K,i} - \sum_{l=1}^{4}\nu_{K,l}X_l}{\nu_{K,K_3AlSi_4O_{10}(OH)_2}} = \frac{0.76 - 0.0867 - 0.0067 - 0.045 - 0.4316}{3}$$

$$= 0.0633. \quad (21)$$

6. Calculate $X_{Al_2Si_4O_{10}(OH)_2}$ from

$$X_{Al_2Si_4O_{10}(OH)_2} = \frac{\nu_{Si,i} - \sum_{l=1}^{5}\nu_{Si,l}X_l}{\nu_{Si,Al_2Si_4O_{10}(OH)_2}} = \frac{3.43 - 3(0.0867) - 3(0.0067) - 3(0.045)}{4} - \frac{3(0.4316) + 4(0.0633)}{4} = 0.3667. \quad (22)$$

CONCLUDING REMARKS

As demonstrated above, illite and smectite solid solutions are two minerals with distinct chemical characteristics that require different sets of thermodynamic components to describe their compositions. Nevertheless, intimate intergrowths of these minerals are commonly represented in the literature by a single chemical formula and referred to as randomly interstratified illite/smectite mixed layer clays. This practice implies that illite and smectite actually exhibit mutual solid solubility, which is not the case. It should, therefore, be avoided. Instead, such clays should be described either as intergrowths or replacement features involving two or more discrete phases.

More and better-constrained TEM/AEM data for single crystals are needed to more closely identify the

https://doi.org/10.1346/CCMN.1993.0410503 Published online by Cambridge University Press

extreme limits of compositional variation in illite and smectite solid solutions as a function of pressure and temperature. Calorimetric studies combined with HRTEM data for single crystals of these minerals are also needed to provide a foundation for describing the thermodynamic behavior and relative stabilities of illite and smectite solid solutions in sedimentary basins. Hopefully, the present communication will stimulate such studies and promote rigorous analysis of the mineralogic, chemical, and textural characteristics of illite and smectite in geologic systems.

ACKNOWLEDGMENTS

The research described above was supported by the National Science Foundation (NSF grants EAR 81-15859, EAR 8606052, and EAR 91-17393), the Department of Energy (DOE contract DE-AT03-83ER-13100 and grant DE-FG03-85ER-13419), and the Committee on Research at the University of California. We are indebted to Everett Shock, Eric Oelkers, Vitalii Pokrovskii, and Jan Amend for helpful discussions and suggestions made during the course of this study. We would like to thank Ray Ferrell Jr. for helpful review comments. We are also grateful to Simon Somers for his computer expertise, Joan Bossart for assistance with word processing, and Peggy Gennaro, Joachim Hampel, Lillian Mitchell, and Kevin Hwang for help in preparing the figures for publication.

REFERENCES

Aagaard, P. and Helgeson, H. C. (1983) Activity/composition relations among silicates and aqueous solutions: II. Chemical and thermodynamic consequences of ideal mixing of atoms on homological sites in montmorillonites, illites, and mixed-layer clays: *Clays & Clay Minerals* **31,** 207–217.

Ahn, J. H. and Peacor, D. R. (1986) Transmission and analytical electron microscopy of the smectite-to-illite transition: *Clays & Clay Minerals* **34,** 165–179.

Bailey, S. W., Brindley, G. W., Fanning, D. S., Kodama, H., and Martin, R. T. (1984) Report of The Clay Minerals Society Nomenclature Committee for 1982 and 1983: *Clays & Clay Minerals* **32,** 239–240.

Brigatti, M. F. and Poppi, L. (1981) A mathematical model to distinguish the members of the dioctahedral smectite series: *Clay Miner.* **16,** 81–89.

Duplay, J. (1984) Analyses chimiques ponctuelles de particules d'argiles. Relations entre variations de compositions dans une population de particles et temperature de formation: *Sciences Geologique Bull.* **37,** 307–317.

Earley, J. W., Osthaus, B. B., and Milne, I. H. (1953) Purification and properties of montmorillonite: *Amer. Mineral.* **38,** 707–724.

Eberl, D. D., Środoń, J., Lee, M., Nadeau, P. H., and Northrop, H. R. (1987) Sericite from the Silverton caldera, Colorado: Correlation among structure, composition, origin, and particle thickness: *Amer. Mineral.* **72,** 914–934.

Eslinger, E., Highsmith, P., Albers, D., and DeMayo, B. (1979) Role of iron reduction in the conversion of smectite to illite in bentonites in the disturbed belt, Montana: *Clays & Clay Minerals* **27,** 327–338.

Foster, M. D. (1951) The importance of exchangeable magnesium and cation-exchange capacity in the study of montmorillonitic clays: *Amer. Mineral.* **36,** 717–730.

Foster, M. D. (1953) Geochemical studies of clay minerals II—Relation between ionic substitution and swelling in montmorillonites: *Amer. Mineral.* **38,** 994–1006.

Foster, M. D. (1954) The relation between "illite," beidellite, and montmorillonite: in *2nd National Conference on Clays and Clay Minerals,* A. Swineford and N. Plummer, eds., *Research Council Pub.* **327,** National Academy of Sciences, Washington, D.C., 386–397.

Garrels, R. M. (1984) Montmorillonite/illite stability diagrams: *Clays & Clay Minerals* **32,** 161–166.

Gaudette, H. E. (1965) Illite from Fond du Lac County, Wisconsin: *Amer. Mineral.* **50,** 411–417.

Gaudette, H. E., Eades, J. L., and Grim, R. E. (1966) The nature of illite: *Clays & Clay Minerals* **13,** 165–166.

Grim, R. E. and Guven, N. (1978) *Bentonites—Geology, Mineralogy, Properties, and Uses:* Elsevier, New York, 256 pp.

Guven, N. (1988) Smectites: in *Hydrous Phyllosilicates Exclusive of Micas,* S. W. Bailey, ed., *Reviews in Mineralogy* **20,** Mineralogical Society of America, Washington, D.C., 497–560.

Heller-Kallai, L. and Rozenson, I. (1981) The use of Mössbauer spectroscopy of iron in clay mineralogy: *Phys. Chem. Minerals* **7,** 223–238.

Holdaway, M. J. (1980) Chemical formulae and activity models for biotite, muscovite, and chlorite applicable to pelitic metamorphic rocks: *Amer. Mineral.* **65,** 711–719.

Hower, J., Eslinger, E., Hower, M. E., and Perry, E. A. (1976) Mechanism of burial metamorphism of argillaceous sediment 1. Mineralogical and chemical evidence: *Geol. Soc. Am. Bull.* **87,** 725–737.

Hower, J. and Mowatt, T. C. (1966) The mineralogy of illites and mixed-layer illite-montmorillonites: *Amer. Mineral.* **51,** 825–853.

Huff, W. D., Whiteman, J. A., and Curtis, C. D. (1988) Investigation of a K-bentonite by X-ray powder diffraction and analytical transmission electron microscopy: *Clays & Clay Minerals* **36,** 83–93.

Inoue, A., Kohyama, N., Kitagawa, R., and Watanabe, T. (1987) Chemical and morphological evidence for the conversion of smectite to illite: *Clays & Clay Minerals* **35,** 111–120.

Inoue, A. and Utada, M. (1983) Further investigations of a conversion series of dioctahedral mica/smectites in the Shinzan hydrothermal alteration area, northeast Japan: *Clays & Clay Minerals* **31,** 401–412.

Inoue, A., Watanabe, T., Kohyama, N., and Brusewitz, A. M. (1990) Characterization of illitization of smectite in bentonite beds at Kinnekulle, Sweden: *Clays & Clay Minerals* **38,** 241–249.

Ireland, B. J., Curtis, C. D., and Whiteman, J. A. (1983) Compositional variation within some glauconites and illites and implications for their stability and origins: *Sedimentology* **30,** 769–786.

Jiang, W. T., Peacor, D. R., Merriman, R. J., and Roberts, B. (1990) Transmission and analytical electron microscopic study of mixed-layer illite/smectite formed as an apparent replacement product of diagenetic illite: *Clays & Clay Minerals* **38,** 449–468.

Kelley, W. P. (1945) Calculating formulas for fine grained minerals on the basis of chemical analysis: *Amer. Mineral.* **30,** 1–26.

Kerr, P. F., Hamilton, P. K., and Pill, R. J. (1950) Analytical data on reference clay minerals: *American Petroleum Institute Project 49, Clay Minerals Standards, Preliminary Report* **7,** 160 pp.

Lee, J. H., Ahn, J. H., and Peacor, D. R. (1985) Textures

https://doi.org/10.1346/CCMN.1993.0410503 Published online by Cambridge University Press

in layer silicates. Progressive changes through diagenesis and low temperature metamorphism: *J. Sed. Petrol.* **55,** 532–540.

Lippmann, F. (1977) The solubility products of complex minerals, mixed crystals, and three-layer clay minerals: *N. Jb. Miner. Abh.* **130,** 243–263.

Lippmann, F. (1982) The thermodynamic status of clay minerals: *Proc. 7th Int. Clay Conf. 1981,* 475–485.

Maniar, P. D. and Cooke, G. A. (1987) Modal analyses of granitoids by quantitative X-ray diffraction: *Amer. Mineral.* **72,** 433–437.

Merino, E. and Ransom, B. (1982) Free energies of formation of illite solid solutions and their compositional dependence: *Clays & Clay Minerals* **30,** 29–39.

Nadeau, P. H. and Bain, D. C. (1986) Compositions of some smectites and diagenetic illitic clays and implications for their origin: *Clays & Clay Minerals* **34,** 455–464.

Nadeau, P. H., Tait, J. M., McHardy, W. J., and Wilson, M. J. (1984a) Interstratified XRD characteristics of physical mixtures of elementary clay particles: *Clay Miner.* **19,** 67–76.

Nadeau, P. H., Wilson, M. J., McHardy, W. J., and Tait, J. M. (1984b) Interparticle diffraction. A new concept for interstratified clays: *Clay Miner.* **19,** 757–769.

Nadeau, P. H., Wilson, M. J., McHardy, W. J., and Tait, J. M. (1984c) Interstratified clays as fundamental particles: *Science* **225,** 923–925.

Newman, A. C. D. and Brown, G. (1987) The chemical constitution of clays: in *Chemistry of Clays and Clay Minerals,* A. C. D. Newman, ed., John Wiley & Sons, New York, 1–128.

Page, R. (1980) *Alteration-mineralization history of the Butte Montana ore deposit and transmission electron microscopy of phyllosilicate alteration phases:* Ph.D. thesis, University of California, Berkeley, 226 pp.

Pawloski, G. A. (1985) Quantitative determination of mineral content of geological samples by X-ray diffraction: *Amer. Mineral.* **70,** 663–667.

Ransom, B. and Helgeson, H. C. (1989) On the correlation of expandability with mineralogy and layering in mixed-layer clays: *Clays & Clay Minerals* **37,** 189–191.

Ransom, B. and Helgeson, H. C. (1993a) A chemical and thermodynamic model of dioctahedral 2:1 layer clay minerals in diagenetic processes: Dehydration of smectite as a function of temperature and depth in sedimentary basins: *Am. J. Sci.* (in press).

Ransom, B. and Helgeson, H. C. (1993b) A chemical and thermodynamic model of dioctahedral 2:1 layer clay minerals in diagenetic processes: Regular solution representation of interlayer dehydration in aluminous smectite: *Am. J. Sci.* (in press).

Reynolds, R. C. (1980) Interstratified clay minerals: in *Crystal Structures of Clay Minerals and Their X-ray Identification,* G. W. Brindley and G. Brown, eds., Mineralogical Society, London, 249–301.

Ross, C. S. and Hendricks, S. B. (1945) Minerals of the montmorillonite group. Their origin and relation to soils and clays: *U.S. Geol. Surv. Prof. Pap.* **205-B,** 23–79.

Schultz, L. G. (1969) Lithium and potassium absorption, dehydroxylation temperature and structural water content of aluminous smectites: *Clays & Clay Minerals* **19,** 137–150.

Środoń, J. (1980) Precise identification of illite/smectite interstratifications by X-ray powder diffraction: *Clays & Clay Minerals* **28,** 401–411.

Środoń, J. and Eberl, D. D. (1984) Illite: in *Micas,* S. W. Bailey, ed., *Reviews in Mineralogy* **13,** Mineralogical Society of America, Washington, D.C., 495–544.

Środoń, J., Morgan, D. J., Eslinger, E. V., Eberl, D. D., and Karlinger, M. R. (1986) Chemistry of illite/smectite and end-member illite: *Clays & Clay Minerals* **34,** 368–378.

Till, R. and Spears, D. A. (1969) The determination of quartz in sedimentary rocks using an X-ray diffraction method: *Clays & Clay Minerals* **17,** 323–327.

Velde, B. and Brusewitz, M. (1986) Compositional variation in component layers in natural illite/smectite: *Clays & Clay Minerals* **34,** 651–657.

Warren, E. A. and Curtis, C. D. (1989) The chemical composition of authigenic illite within two sandstone reservoirs as analyzed by ATEM: *Clay Miner.* **24,** 137–156.

Warren, E. A. and Ransom, B. (1992) The influence of analytical error upon the interpretation of chemical variations in clay minerals on standard clay diagrams AEM and XRD: *Clay Miner.* **27,** 193–209.

Weaver, C. E. and Pollard, L. D. (1973) *The Chemistry of Clay Minerals:* Elsevier, New York, 213 pp.

Weir, A. H. (1965) Potassium retention in montmorillonites: *Clay Miner.* **6,** 17–22.

Yau, Y., Peacor, D. R., and McDowell, S. D. (1987) Smectite-to-illite reactions in Salton Sea shales: A transmission and analytical electron microscopy study: *J. Sed. Petrol.* **57,** 335–342.

Yoder, H. S. and Eugster, H. P. (1955) Synthetic and natural muscovites: *Geochim. Cosmochim. Acta* **8,** 255–280.

(Received 5 September 1991; accepted 11 February 1993; Ms. 2141)

https://doi.org/10.1346/CCMN.1993.0410503 Published online by Cambridge University Press